A New Approach to Structural Failure Detection Based on Adaptive Lattice Filtering

Sanjay S. Joshi*and David S. Bayard†
Jet Propulsion Laboratory
California Institute of Technology
4800 Oak Grove Drive, Pasadena, CA 91109

Abstract

A new approach to structural failure detection and localization is introduced based on acoustic reflections. It is shown that the cross-sectional areas of structural elements can be computed directly in terms of the reflection coefficients of an optimal finite impulse response Wiener filter realized in lattice form. This leads to an elegant method to detect and localize structural failures using recursive on-line estimation rncthods. There are many advantages of this approach relative to standard failure detection schemes. Specifically, the acoustic reflection approach: 1) dots not require training; 2) does not require prior knowledge of a structural model; 3) can detect and localize multiple failures; 4) can indicate the extent of damage at each location. A simulation example is given which successfully demonstrates each of these qualities.

For the present paper, tbc acoustic reflection method is established by working out the theory completely for a bar with nonuniform cross-sectional area in axial vibration. Some ideas for extending the theory to more elaborate and realistic structural configurations arc briefly outlined.

1 Introduction

A new approach to structural failure detection and localization is introduced based on acoustic reflections. The basic idea is to "ping" the structure and construct a map of the reflected energy. This acts as a signature which can be monitored to detect future changes in the structure. More importantly, it is shown that the location of the failure and *extent of damage* can be estimated by using the wave propagation and reflection properties of the structure which are inevitably changed in the location of the failure.

It is a main result of the paper that key reflectivity properties for detection and localization of changes in a structural element obeying second-order wave propagation dynamics (i .c., a bar in axial vibration or a shaft in torsional vibration) are characterized systematically and elegantly in terms of the reflection coefficients of an optimal finite impulse response (FIR) Wiener filter implemented in lattice form. This is important since many practical on-line methods are available for estimating the optimal Wiener FIR filter. For example, recursive implementations are known using the LMS algorithm [1 7], or faster methods using adaptive lattice forms [23] and/or recursive least squares adaptation [19] [22]. Such implementations also do not restrict the input excitation, i.e., instead of an impulsive "pinging" of the structure, the required information can be obtained in a more gentle fashion try using low-level broad-band input excitation correlated over long periods of time.

•Member of ~'ethnical Staff, Guidance and Control Section; also Research Assistant, School of Engineering, UCLA.

'Member of Technical Staff, Guidance and Control Section and Corresponding Author.

The reflectivity method provides the capability to detect and localize a failure without the tedious task of training a optimal or suboptimal detector/classifier. The importance of this property can be appreciated by noting that it is usually impossible to train on actual faults since they must be implemented physically to elicit the proper signatures, Alternatively, fault signatures can be obtained by computer simulation or by analytical methods. However, this latter approach requires an accurate model of the system parametrized in physically meaningful coordinates. It is questionable whether such a model exists in most applications of interest, or if the fidelity would be sufficiently high to permit accurate detection/localization. The reflectivity method dispenses with the need to train using fault signatures, or the need for an accurate physical model. The reflectivity approach can also detect and localize multiple simultaneous faults, and can provide relative information about the extent of damage at each location.

Pulse reflectivity methods have been used successfully in detecting breaks in electrical transmission lines [16], in detecting faults in optical fibers [15], in determining physical properties of materials using ultrasound [14], and in determining cross-sectional areas of the vocal tract using acoustic tube models []]. However, to the authors' knowledge such approaches have not yet been applied to FDI in structures. The present paper is focused to help fill this gap. In this paper, the theory of acoustic reflections is worked out completely for a bar with nonuniform cross-sectional area, Extension to fourth-order systems (such as a beam in bending vibration) and to complex interconnected structures is an area for future research, but some reasonable approaches will be briefly outlined.

The paper is organized as follows. In Section 2, the optimal FIR Wiener filter is derived, and its lattice realization in terms of reflection coefficients is discussed. In Section 3, the wave propagation properties of a bar are derived in terms of reflection properties and cross sectional areas, and a similar lattice type of recursion is derived. In Section 4, the lattice recursions for both the optimal Wiener filter and structural element are equated. This leads to the main result of the paper which shows that the cross-sectional areas of the stuctural element can be computed directly in terms of reflection coefficients. Hence, changes in the structure can be detected and localized completely in terms of the optimal Wiener filter, which in turn can be estimated recursively on-line. A simulation example is given in Section 5 to demonstrate the advantages and usage of the approach, further research directions are outlined in Section 6, and conclusions are postponed until Section 7. Additional supporting material and analysis can be found in the appendices.

2 Lattice Realization of an Optimal FIR Filter

Consider the following inverse filtering problem. Let a discrete, FIR *inverse* transfer function of a system be defined as

$$Q(z) = \frac{P(z)}{U(z)} = 1 + \sum_{k=1}^{M} \alpha(k) z^{-k} \tag{1}$$

It is clear that the inverse transfer function can be completely specified with the knowledge of the parameters $\alpha(1),\alpha(2),\ldots.\alpha(M)$. If only input/output data of the system is available, the unknown parameters may be identified using a least squares estimation procedure to obtain an optima] transfer function for the given data. This represents the optimal FIR Wiener filter [1 7]. This optimal transfer function maybe implemented in a variety of ways. One widely used realization in adaptive filtering is the lattice filter realization. The lattice filter is implemented in a series of M stages for an M^{th} order FIR filter. The first stage accepts the input to the

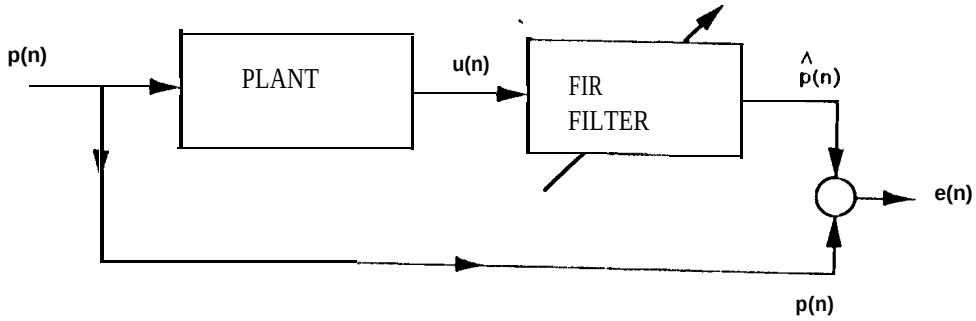

Figure 1: Inverse Filtering Problem

filter and the M^{th} stage produces the output of the filter. Pictorially, it is shown as Figure 2. Note that the first stage receives two inputs, both of which are the filter input. Two quantities,

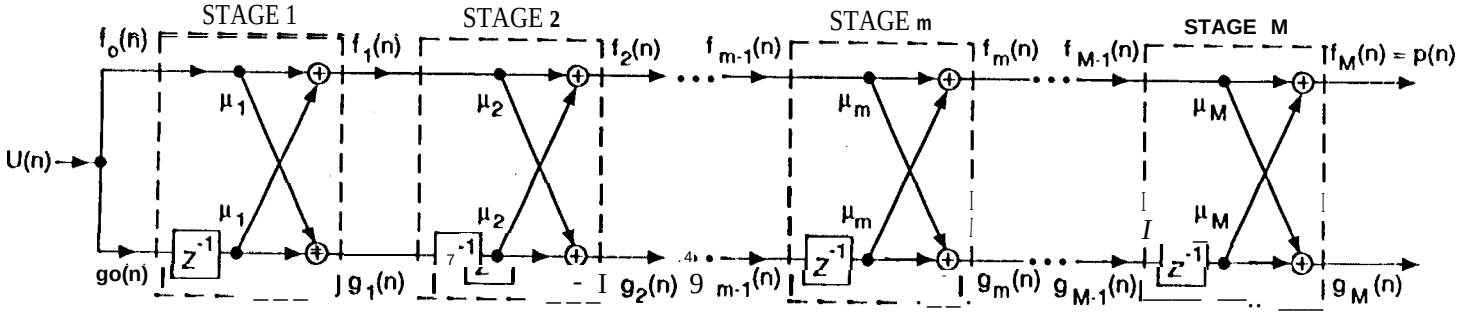

Figure 2: Stages of a Lattice Filter

$f(n)$ and $g(n)$ are recursively updated after each stage. After stage M, $f(n)$ becomes the filter Output, (n).

The lattice filter is described by the following set of well known order-recursive equations [2]

$$f_0(n) = g_0(n) = u(n) \tag{2}$$

$$f_m(n) = f_{m-1}(n) + \mu_m g_{m-1}(n-1) \quad m = 1, 2, \ldots, M \tag{3}$$

$$g_m(n) = \mu_m f_{m-1}(n) + g_{m-1}(n-1) \quad m = 1, 2, \ldots M \tag{4}$$

$$p(n) = f_M(n) \tag{5}$$

The μ_m's in the update are called *reflection coefficients* of the filter. There are several ways to

calculate the reflection coefficients given the α parameters. Some of the ways are explained in [2].

Let $Q_M^+(z)$ be the inverse transfer function of the system corresponding to (1). It can be shown (*Appendix A*) that $Q_M^+(z)$ may be recursively calculated using the matrix recursion,

$$\begin{bmatrix} Q_m^+(z) \\ Q_m^-(z) \end{bmatrix} = \begin{bmatrix} 1 & -\mu_m \\ -z^{-1}\mu_m & z^{-1} \end{bmatrix} \begin{bmatrix} Q_{m-1}^+(z) \\ Q_{m-1}^-(z) \end{bmatrix} \tag{6}$$

Where

$$Q_0^+(z) = 1 \qquad Q_0^-(z) = -z^{-1}$$

3 A Recursive Solution to the Bar Equation

A solution will now be examined for the axial wave equation in a bar. We assume that the bar is lossless and admits perfect reflection at one end. It will be shown that a bar can be thought of as being composed of several stages just. as in a lattice filter. As a result, a recursive solution for the inverse transfer function of the bar can be. derived which is very much like the one derived for the lattice filter. In addition, the reflection coefficients of the recursive solution now take on a physical significance that is very useful for structural failure detection and localization.

Let $u(x,t)$ be the axial displacement of a bar element, where x is the distance variable in the axial direction and t is the time variable. For an axial bar element in which plane waves before deformation remain plane, $u(x,t)$ satisfies the wave equation given by

$$EA\frac{\partial^2 u(x,t)}{\partial x^2} = \rho A \frac{\partial^2 u(x,t)}{\partial t^2} \tag{7}$$

In this equation, E is the elastic modulus, A is the cross sectional area, and ρ is the mass density. This equation has the traveling wave solution

$$u(x,t) = u^+\left(t - \frac{x}{c}\right) - u^-\left(t + \frac{x}{c}\right) \tag{8}$$

where c is the wave speed given by $c = \sqrt{\frac{E}{\rho}}$. Equation (8) can be interpreted as the summation of two waveforms traveling in opposite directions. in particular, the waveform traveling to the right is denoted as $u^+\left(t - \frac{x}{c}\right)$ and the one traveling to the left, is denoted by $u^-\left(t + \frac{x}{c}\right)$.

The entire! bar is now represented as a series of axially connected bars called sections of cqu al length, *61*. Section *M* represents the far left hand section and section 1 is the far right hand section. Between each section is a boundary. From structural theory, both the displacement and the axial force must be continuous at each boundary. The axial force is related to the displacement wave by $p(x,t) = EA\frac{\partial u(x,t)}{\partial x}$. Let $u_{m+1}^+(t)$ and $u_{m+1}^-(t)$ be the forward and backward displacement waves measured directly *at boundary* $m+1$ *and time* t. By using the boundary conditions and the properties of a 1oss1css bar, it is shown in *Appendix B* that $u_{m+1}^+(t)$ and $u_{m+1}^-(t)$ can be related to the displacement waves measured at boundary m, $u_m^+(t)$ and $u_m^-(t)$, as follows

$$u_{m+1}^-(t + \delta t) = \frac{1}{1+\eta_m}[u_m^-(t) - \eta_m u_m^+(t)] \tag{9}$$

and

$$u_{m+1}^+(t - \delta t) = \frac{1}{1+\eta_m}[u_m^+(t) - \eta_m u_m^-(t)] \tag{10}$$

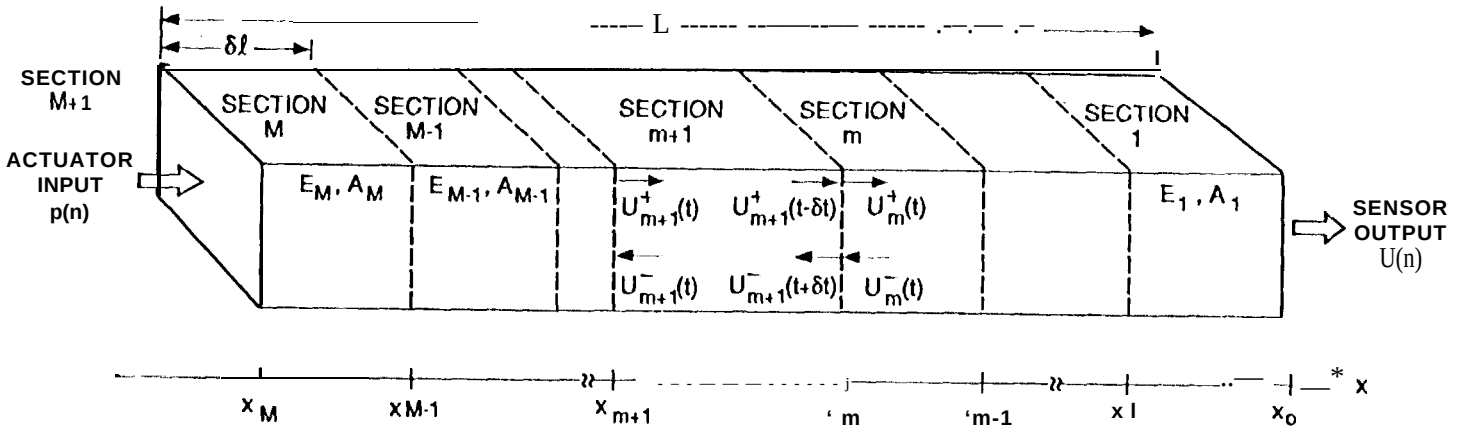

Figure 3: Bar Element Composed of M Stages

where

$$\eta_m \triangleq \frac{E_{m+1}A_{m+1} - E_mA_m}{E_{m+1}A_{m+1} + E_mA_m} \triangleq \frac{S_{m+1} - S_m}{S_{m+1} + S_m} \tag{11}$$

In this equation, & is the time required for a wave to travel through one section of the bar, given by $\delta t = \frac{\delta l}{c}$; E_{m+1} is the elastic modulus of section m + 1; A_{m+1} is the cross sectional area of section $m+1$; and S_m is defined as $S_m \triangleq E_mA_m$.

Let z be defined as

$$z \triangleq e^{j\omega(2\delta t)} = e^{j\omega 2\frac{\delta l}{c}}$$

Then, by taking the z transform of (9) and (10) where $U^-_{m+1}(z)$ represents the z transform of $u^-_{m+1}(t)$ and $U^+_{m+1}(z)$ represents the z transform of $u^+_{m+1}(t)$

$$\begin{bmatrix} U^+_{m+1} \\ U^-_{m+1} \end{bmatrix} = \frac{z^{\frac{1}{2}}}{1+\eta_m} \begin{bmatrix} 1 & -\eta_m \\ -\eta_m z^{-1} & z^{-1} \end{bmatrix} \begin{bmatrix} U^+_m \\ U^-_m \end{bmatrix} \tag{12}$$

As a result of perfect reflection at the right end of the bar, η_0 takes a value of 1. Therefore, for section 1, (12) may be written as

$$\begin{bmatrix} U^+_1 \\ U^-_1 \end{bmatrix} = \frac{z^{\frac{1}{2}}}{1+\eta_0} \begin{bmatrix} 1 & -1 \\ -z^{-1} & z^{-1} \end{bmatrix} \begin{bmatrix} U^+_0 \\ U^-_0 \end{bmatrix} = \frac{z^{\frac{1}{2}}}{1+\eta_0} \begin{bmatrix} 1 \\ -z^{-1} \end{bmatrix} \{U^+_0 - U^-_0\} \tag{13}$$

Furthermore, by repeatedly applying (1 2), the following relation is obtained for any section $m+1$,

$$\begin{bmatrix} U^+_{m+1} \\ U^-_{m+1} \end{bmatrix} = (z^{\frac{1}{2}})^{m+1} \prod_{k=0}^{m} \frac{1}{1+\eta_k} \begin{bmatrix} 1 & -\eta_m \\ -z^{-1}\eta_m & z^{-1} \end{bmatrix} \cdots \begin{bmatrix} 1 & -\eta_1 \\ -z^{-1}\eta_1 & z^{-1} \end{bmatrix} \begin{bmatrix} 1 \\ -z^{-1} \end{bmatrix} \{U^+_0 - U^-_0\} \tag{14}$$

Now define

$$\begin{bmatrix} D^+_m(z) \\ D^-_m(z) \end{bmatrix} \triangleq \begin{bmatrix} 1 & -\eta_m \\ -z^{-1}\eta_m & z^{-1} \end{bmatrix} \cdots \begin{bmatrix} 1 & -\eta_1 \\ -z^{-1}\eta_1 & z^{-1} \end{bmatrix} \begin{bmatrix} 1 \\ -z^{-1} \end{bmatrix} \tag{15}$$

and

$$K_m \triangleq \prod_{k=0}^{m} \frac{1}{1+\eta_k} \tag{16}$$

Equation (14) is now written as

$$\begin{bmatrix} U_{m+1}^{+} \\ U_{m+1}^{-} \end{bmatrix} = (z^{\frac{1}{2}})^{m+1} K_m \begin{bmatrix} D_m^{+} \\ D_m^{-} \end{bmatrix} \{U_0^{+} - U_0^{-}\} \tag{17}$$

Normalizing equation (17) by K_m and defining $N_{m+1}^{+} \triangleq \frac{U_{m+1}^{+}}{K_m}$ and $N_{m+1}^{-} \triangleq \frac{U_{m+1}^{-}}{K_m}$,equation (17) can be written as

$$\begin{bmatrix} N_{m+1}^{+} \\ N_{m+1}^{-} \end{bmatrix} = (z^{\frac{1}{2}})^{m+1} \begin{bmatrix} D_m^{+} \\ D_m^{-} \end{bmatrix} \{U_0^{+} - U_0^{-}\} \tag{18}$$

Let $H_M^{+}(z)$ be the inverse transfer function of the bar,

$$H_M^{+}(z) \triangleq \frac{N_{M+1}^{+}(z)}{U_0^{+}(z) - U_0^{-}(z)} \tag{19}$$

It is defined as the ratio of the displacement wave at the far left of the bar over the displa.cement wave at the far right of the bar. However, to represent the boundary conditions at the far left of the bar in the same way as the boundary conditions at each junction in the bar, an imaginary section $M + 1$ canbe visualized that has a matching impedance to section *M.* As a. result of the matched impedance, there is no negative traveling wave in section *M*+- 1. *Then,* the input may be applied in section $M + 1$ and the boundary condition at junction *M* can be stated in terms of a reflection coefficient. In this scheme, an extra $z^{\frac{1}{2}}$ delay is also artificially created. It is assumed, though, that the input is added at the far left of the bar, so the added delay may be removed.

By using the definition of H_M^{+} (z), the inverse transfer function bet wcen any section m and the front end can be described as

$$H_m^{+}(z) \triangleq \frac{N_{m+1}^{+}(z)}{U_0^{+} - U_0^{-}(z)} \tag{20}$$

Similarly, we may define

$$H_m^{-}(z) \triangleq \frac{N_{m+1}^{-}(z)}{U_0^{+} - U_0^{-}(z)} \tag{21}$$

by using the backward moving displacement wave. Substituting (20) and (2 I) into (18) yields,

$$\begin{bmatrix} H_m^{+}(z) \\ H_m^{-}(z) \end{bmatrix} = (z^{\frac{1}{2}})^{m+1} \begin{bmatrix} D_m^{+}(z) \\ D_m^{-}(z) \end{bmatrix} \tag{22}$$

The fin al form inverse transfer function is then,

$$H_M^{+}(z) = \frac{N_{M+1}^{+}}{U_0^{+} - U_0^{-}} = (z^{\frac{1}{2}})^{M+1} D_M^{+}(z) \tag{23}$$

where $D_M^{+}(z)$ is solved using (1 5). Then, by removing the extra $z^{\frac{1}{2}}$ delay,

$$\frac{U_{M+1}^{+}}{U_0^{-} - U_0^{+}} = (z^{\frac{1}{2}})^{M} K_M D_M^{+}(z) \tag{24}$$

The z term represents a delay and the K_M is a gain factor.

Note that $D_m(z)$ in equation (15), may be put in recursive form by taking,

$$\begin{bmatrix} D_{m+1}^{+}(z) \\ D_{m+1}^{-}(z) \end{bmatrix} = \begin{bmatrix} 1 & -\eta_{m+1} \\ -\eta_{m+1} z^{-1} & z^{-1} \end{bmatrix} \begin{bmatrix} D_m^{+}(z) \\ D_m^{-}(z) \end{bmatrix} \tag{25}$$

where

$$D_0^{+}(z) = .1 \qquad D_0^{-}(z) = -z^{-1}$$

This recursion form is the same as that derived for a FIR filter with a lattice realization (6).

4 Identifying Damage Extent and Location

A recursive solution for an inverse transfer function was shown in equation (6) through the use of a lattice filter. By way of a completely separate physical argument., a recursive solution for the inverse transfer function for a bar element was shown in equation (25). By comparing these equations, it is clear that the two solutions are equivalent. This provides a physical justification for modeling the inverse transfer function of a bar as a FIR filter. Furthermore, the reflection coefficients generated take on a physical meaning as defined in equation (11).

As a result of the above equivalence, a procedure may now be developed to estimate the cross sectional areas of a bar. First, by using input/output data from a bar, the optimal, FIR inverse transfer function is identified. 'l'he bar is now represented as a series of M sections and the reflection coefficient, η_m, for each section is calculated as in a lattice filter. It should be noted that the total number of bar sections, M, is constrained by the sampling period of the output data. collection. Recall the equivalence of the recursive solutions of the FIR filter and the bar element was shown when

$$z = e^{j\omega T} = e^{j\omega 2\frac{\delta l}{c}} \tag{26}$$

where T is the sampling period. Since the sampling period is defined when taking data,

$$\delta l = \frac{Tc}{2} = \frac{1}{2}T\sqrt{\frac{E}{\rho}} \tag{27}$$

and the total number of sections is constrained to $M = \frac{L}{\delta l}$ where L is the total length of the bar. The reflection coefficients are now used to recursively calculate the cross sectional areas of the bar. From equation (11);

$$S_m = \frac{1-\eta_m}{1+\eta_m}S_{m+1} \tag{28}$$

Since the E's are assumed equal and constant,

$$An, = \frac{1-\eta_m}{1+\eta_m}A_{m+1} \tag{29}$$

Note that the actual cross sectional area at boundary x_M, the far left side of the bar, is needed to start the recursion. If, however, this area is not known, it may be taken as 1. In this case, all areas estimated will be normalized and damage will appear as a *change* in estimated normalized areas. As a result, failure can still be identified and localized, but the exact amount cannot be determined. Since η_0 is taken to be 1, the area at boundary x_0, the far right side of the bar, cannot be estimated. Therefore, this procedure estimates cross sectional areas at all boundary points except for the endpoints.

It is clear from equation (29) that the reflection coefficient at the far left side of the bar, η_M, is never used in the estimation of the cross sectional areas. Also, it is noted that all reflection coefficients, η_m, are dependent only on structural characteristics on either side of a single boundary (11). As a result, the estimation procedure is *independent* of the boundary condition on the far left side of the bar. This eliminates the need for knowledge of material properties of adjoining structural sections. Note, however, that although it is never used, η_M is estimated. This immediately gives us information about the structural properties of the adjoining section at the far left of the bar.

Ideally, the cross sectional areas of the bar are continuously calculated. When some damage dots occur, cross sectional areas change and the extent and location of the damage is immediately known. Note that if damage occurs between two boundary locations, both the estimated cross sectional areas at the boundary before and after the damage location will change. This wil isolate the damage location between two boundary points.

5 Simulation Example

The acoustic reflection method is now illustrated through the use of a simulation example. Consider a uniform 3 meter bar made of structural steel with cross sectional area of .00129 m^2 (2 in^2). The setup is shown in Figure 4. On the far left side of the bar is a stack of piezoelectric

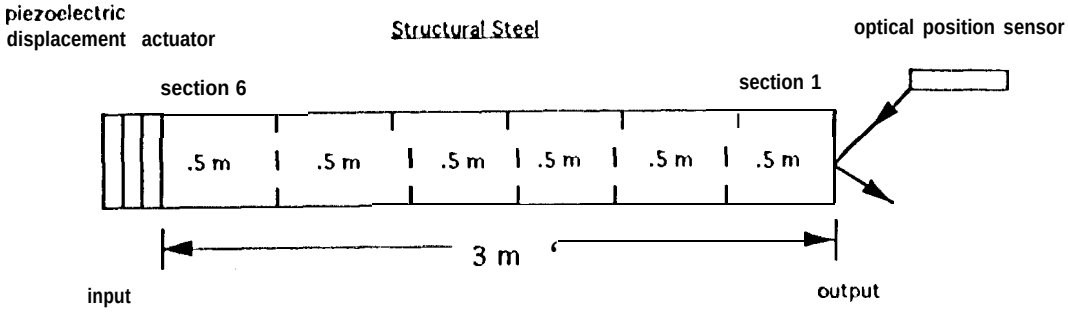

Figure 4: Simulated Experimental Setup for Acoustic Reflection Method

actuators that are capable of commanding displacement. On the far right of the bar is a laser displacement sensor. Structural steel has an elastic modulus, E, of 2el $1N/m^2$ and a density, ρ, of 7870 kg/m^3. We take the sampling rate of the sensor to be 5041.127 Hz. This sampling rate determines the sectional length (27) as .5 meters. Since the total length of the bar is 3 meters, we have a total of 6 sections.

Any input can be applied by the displacement actuator in this method. For illustration purposes, assume a .001 meter impulse is applied. The impulse response of the uniform bar (undamaged) is shown in Figure 5. Note that the horizontal axis is marked in normalized time, Each time unit represents the time required for a wave to travel through two sections of the bar. In this case, this time is .198 ms. As can be seen, the first output appears at time unit 3. This pure delay is the time required for the impulse to travel through all 6 sections of the bar.

The optimal FIR filter is identified using a least squares procedure described in *Appendix B*. From this optimal FIR filter, reflection coefficients and cross sectional areas are estimated. We assume that wc know the cross sectional area of the far left of the bar exactly as .00129 m^2. If this area. were not known, it could bc taken as 1 and normalized areas could be calculated. The estimated bar is also shown in Figure 5. The crosshatched bars represent the simulated areas of each section. The white bars represent the estimated areas using only input/output data. Note that no damage appears and all cross sectional areas are estimated to be equal. The bar is now simulated to be damaged at section 3 such that the cross sectional area in that section has been reduced by 50%. The new impulse response and the estimated damage is shown in Figure 6. Note that the estimated damage of section 3 is exactly 1/2 the original area of the section. To show that the method works for small values of damage as well as large values, the bar is simulated such that section 3 is 95 % of its original area. Again, using only input/output data, the cross sectional areas are estimated. The results are shown in Figure 7.

Finally, the method is shown on multiple failures. The bar is simulated such that section 2 is 60 % of its original area, section 3 is 70% of its original area, and section 5 is 50 % of its original area. The impulse response and the estimated damage is shown in Figure 8. The method works well for several failures at once.

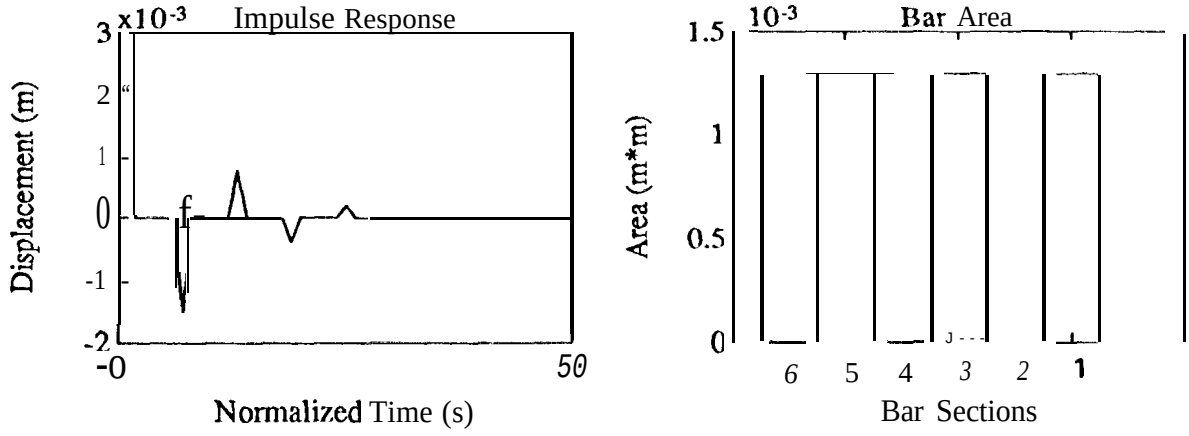

Figure 5: Estimation of Cross-sectional Area of Uniform Bar ($1.29e\text{-}3\,m^2$) with Acoustic Reflection Method

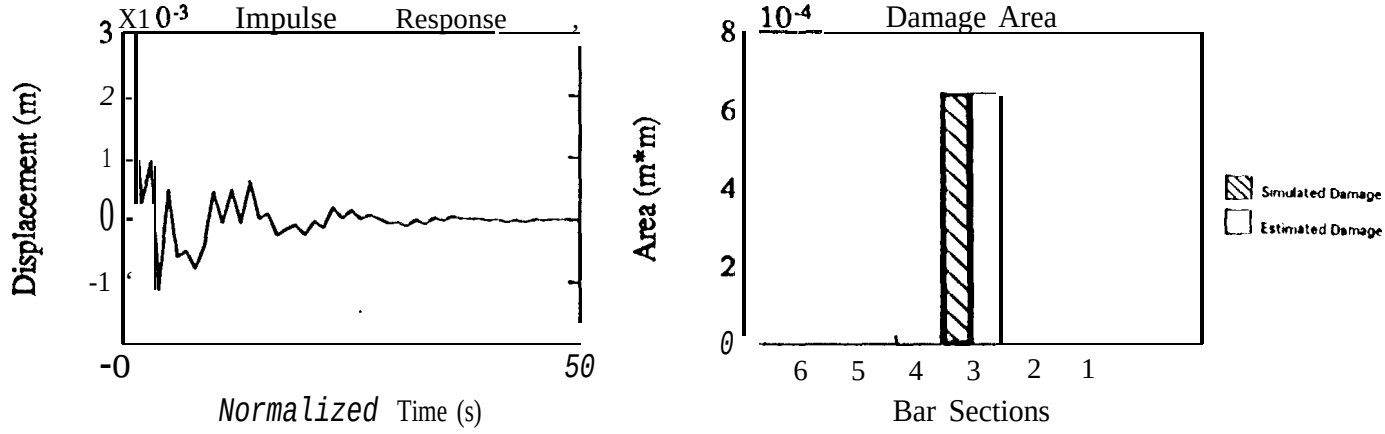

Figure 6: Detection, Localization, and Estimation of Change in Cross-sectional Areas- 50 % Change in Section 3

We have simulated the acoustic reflection method on an ideal bar to demonstrate the approach. However, in actual experimentation, there arc several issues that must be considered. First, noise corrupts all measurements. As a result, estimated areas will be incorrect to some degree and noll-existent damage may appear. This is particularly troublesome when trying to identify small amounts of damage. Therefore, some sort of threshold will be needed. Secondly, the FIR model order may cause potential difficulty. The model order is fixed in this method by the sampling rate. However, if this model order is not high enough to accurately model the bar, estimated areas may be incorrect. This problem may be overt.omc by increasing the sampling rate. Finally, the accuracy of the system identification techniques must be considered. System identification techniques use data that is inevitably corrupted by measurement noise and round-off error. As a result, it is important to use enough data such that these effects can be minimized when filter parameters arc identified.

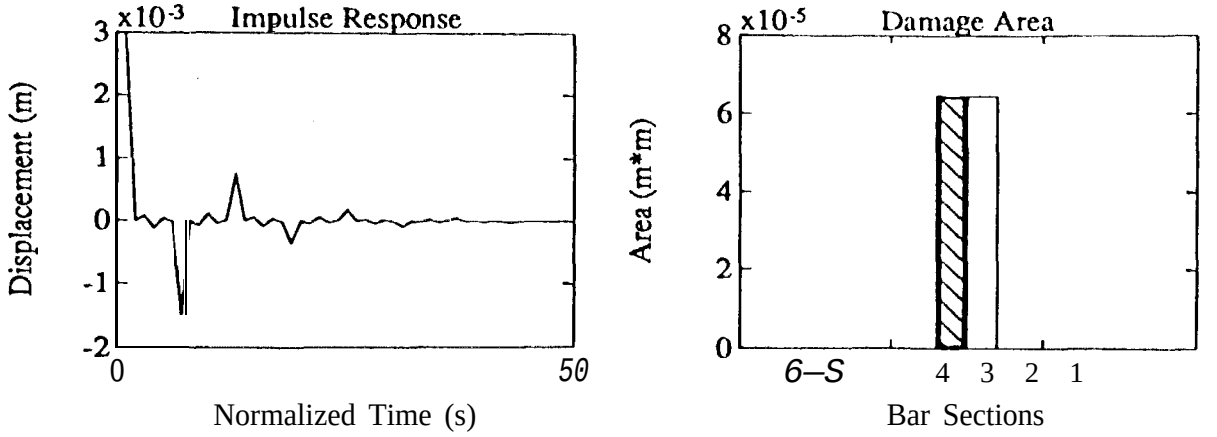

Figure 7: Detection, Localization, and Estimation of Change in Cross-sectional Areas- 5 % Change in Section 3

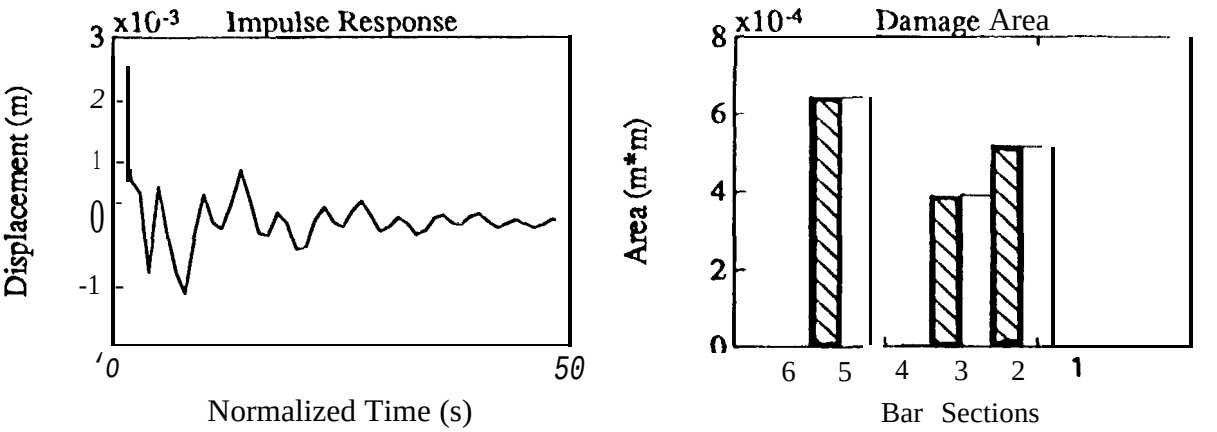

Figure 8: Detection, Localization, and Estimation of Change in Cross-sectional Areas- 40 % Change in Section 2, 30 % Change in Section 3, 50 % Change in Section 5

6 Further Work

As derived herein, the acoustic reflection method can be applied to fault detection in second order systems such as a string in transverse vibration, a bar in axial vibration, or a shaft in torsional vibration. An important future extension would be the application to fourth order systems such as a beam in bending vibration. It is known that such systems have traveling wave representations [18][1 I]. However, in fourth order systems the medium is dispersive and the wave changes shape as it travels. This would generally require a more complicated analysis, e.g., the use of pole-zero lattices (e.g., [20] [21]) or heavily overparametrized all-pole lattice representations [23]. Alternatively, the dispersive qualities of the structure could be minimized by restricting the excitation to wave packets over restricted narrowbands of frequency, or by using colocated actuator/sensor instrumentation with time-windowing to retain only the early portion of the pulse response (i.e., the near-field return).

The extension to a complete structure with interconnected elements is also desired. Much of the groundwork for this extension has already been laid due to recent efforts directed at controlling structures based on traveling wave representations [10][11][1 2][13]. Here, each structural element is considered to be a waveguide, and the energy reflection properties at the junctions

(boundaries) are represented by scattering matrices. The scattering matrix concept generalizes the notion of a reflection coefficient used to characterize a one-dimensional boundary. Representing each structural member as a lattice filter, it is conceivable that an "3-D lattice model" of the structure can be built by interconnecting lattice filters with the same geometry as the true structure, using the appropriate scattering matrix interconnections at the boundaries. A long term goal would be to estimate cross-sectional areas at each point of the 3-dimensional lattice model using actuators and sensors distributed about the structure.

The analysis in this paper utilized a displacement wave representation of the dynamics. An important alternative would be to consider "force-velocity" representations. This gives a perfect analogy to "voltage-current" representations of transmission lines, and "pressure-volume velocity" representations of acoustic waveguides. Powerful network analysis methods could then be applied, and "impedance" concepts could be developed. It appears that such an approach would lend more insight into the treatment of boundary conditions, and would be most useful for extending the theory to interconnected structures.

While extending the method as outlined above requires additional research effort, a simple brute! force. method which would work for any structure or configuration would be to treat the detection problem as a pattern recognition problem, and usc the estimated cross-sectional areas (derived from the reflection coefficients) as "feature vectors". To the authors' best knowledge, such physically motivated features have not yet been used for detection/localization in structures. It seems that the cross-sectional area estimates would make very good feature vectors since they enjoy a one-to-one correspondence to fault locations in second-order systems under ideal conditions, and hence would at least correlate strongly with the location of faults for more complex interconnected fourth order systems.

7 Conclusions

A method for structural failure detection and localization has been introduced based on acoustic reflections. The theory has been worked out completely for a bar with nonuniform cross-sectional area. An important theoretical result is that the cross-sectional areas of the bar can be calculated directly in terms of the reflection coefficients of the optimal FIR Wiener filter realized in lattice form. This reduces the problem of detecting and localizing failures to one of estimating the optimal FIR Wiener filter for the inverse plant. Fortunately, many convenient recursive algorithms exist for estimating the optimal FIR Weiner filter and any of such methods can be used with the present approach.

A simulation study was conducted to validate the overall acoustic reflection approach. A uniform bar was chosen as the structural clement for the study. The cross-sectional areas of the bar were perturbed to various extents in multiple locations to simulate structural failures and damage of various extent. *As expected from the theory, the acoustic reflection algorithm correctly detected and located multiple failures in the bar, and estimated the extent of* damage at *each location. Furthermore, as expected from the theory, it accomplished this without training, and without prior knowledge of a structural model.*

The results of this study arc very encouraging, and indicate various directions for future efforts. 'J'he most obvious are extension to fourth-order systems, and extensions to interconnected systems. While such extensions arc not straightforward, some guidelines and possible approaches were discussed in the paper.

Acknowledgements

This research was performed at the Jet }'repulsion laboratory, under contract with the National Aeronautics and Space Administration. This research was partially supported by the

References

[1] Wakita, H., "Direct Estimation of the Vocal Tract Shape by inverse Filtering of Acoustic Speech Waveforms," *IEEE Transactions on Audio and Electronics*, vol. AU-21, No. 5, October, 1973, pp. 417-426.

[2] Proakis, J .G. and Manolakis, D.G., *Introduction to Digital Signal Processing*, Macmillan Publishing Company, 1988.

[3] Roberts, R. A. and Mullis, C.T.,*Signal Processing*, Addison- Wesley Publishing Co., 1987.

[4] Meirovitch, 1,., *Analytical Methods* in *Vibrations*, Macmillan Company, 1967.

[5] Kuehnle, A .U. ,"Control of Longitudinal Waves in a Rod with Voigt Damping," *Proceedings of the American Controls Conference, 1989,* Pittsburgh, PA, June, 1989, pp.200-205.

[6] Fujii, 11. and Ohtsuka, T., "Experiment of a Noncollocated Controller for Wave Cancellation," *Journal of Guidance, Control, and Dynamics,* Vol. 15, No.3, May-June 1992, pp.741-745.

[7] Chen, J.C. and Garba, J, A., "On Orbit Damage Assessment for Large Space Structures" ,*Proceedings of the A IA A/A SME/A SCE/A HS 28th Structures, Structural Dynamics, and Materials Conference*,April 1987.

[8] Hajela, P. and Soeiro, F. J.,''Structural Damage Detection Based on Static and Modal Analysis," *AIAA Journal*, Vol. 28, No. 6,June, 1990, pp. 1110-1115.

[9] Kabe, A.M.,''Stiffness Matrix Adjustment Using Modal Data," *AIAA Journal*,Vol. 23, No. 9, September , 1985, pp. 1431-1436.

[10] A .11. Von Flotow, 'l'raveling wave control for large space structures," J. Guidance, Control and Dynamics, vol. 9, no. 4, pp. 462-468, 1986.

[11] A .H. Von Flotow, "Disturbance propagation in structural networks," J. Sound and Vibration, vol. 106, no. 3, pp. 433-450, 1986.

[12] All. Von Flotow and B. Schafer, "Wave-absorbing controllers for a flexible beam ," J. Guidance, Control, and Dynamics, vol. 9, no. 6, pp. 673-680, 1986.

[13] D.W. Miller and A.H. Von Flotow, "A traveling wave approach to power flow in structural networks," J. Sound and Vibration, vol. 128, no. 1, pp. 145-162, 1989,

[14] D.J. McClements and P. Fairley, "Ultrasonic pulse echo reflectometer," Ultrasonics, vol. 29, pp. 58-62, January 1991.

[15] S. Hangai and Y. g'ski, "Detection of faults in short fiber by the phase compensated reflectometer," IEEE 'bans. Instrumentation and Measurement, vol. 39, no. 1, pp. 238-241, February 1990.

[]6] L.P. Van Biesen, J. Renneboog, and A.R.F. Barel, "High accuracy location of faults on electrical lines using digital signal processing," IEEE Trans. lnstrurnentation and Measurement, vol. 39, no. 1, pp. 175-179, February 1990.

[17] B. Widrow and S.D. Stearns, *Adaptive Signal* Processing. Prentice-Hall, Englewood Cliffs, N. J., 1985.

[18] M. Zac, "Dynamical response to pulse excitations in large space structures," in *Large Space Structures: Dynamics* and *Control*, S.N. Atluri, A .K. Amos (Eds.), Springer-Verlag, Gerlin 1988.

[19] B. Friedlander, "Lattice filters for adaptive processing," Proc. IEEE, vol. 70, pp. 829-867, 1982.

[20] F. Jabbari and J.S. Gibson, "Vector-channel lattice filters and identification of flexible structures," IEEE Trans. Automatic Control, vol. *33,* no. *5,* pp. 448-456, May 1988.

[21] F. J abbari and J.S. Gibson, "Adaptive identification of a flexible structure by lattice filters< AIAA J. Guidance, Control and Dynamics, pp. 548-554, July-August, 1989.

[22] D.M. Wiberg, "Frequencies of vibration estimated by lattices," J. Astronautical Sci., vol. 33, pp. 35-47, 1985.

[23] J. Makhoul, "Linear prediction: A tutorial review," Proc. IEEE, vol. 63, pp. "561-580, April 1975.

APPENDIX A

Least Squares Estimation and the Lattice Realization

Let an inverse transfer function be defined as

$$Q(z) = 1 + \sum_{k=1}^{M} \alpha(k) z^{-k} \tag{30}$$

It is clear that the inverse transfer function is an FIR filter with parameters $\alpha(1), \alpha(2), \ldots, \alpha(M)$. There are M unknown α's needed to characterize the transfer function. The unknown parameters are identified using a least squares estimation procedure. Denote the error between the measured $p(n)$ and that estimated from our model as e(n). Then

$$e(n) = p(n) - \sum_{k=0}^{M} \alpha(k) u(n-k); \qquad \alpha(0) = 1 \tag{31}$$

The sum of the squares of the errors from time, O, to the current time, n, is written

$$E(n) = \sum_{t=0}^{n} e^2(t) = \sum_{t=0}^{n} \{p(t) - \sum_{k=0}^{M} \alpha(k) u(t-k)\}^2 \tag{32}$$

where t is a discrete variable. $E(n)$ is now minimized with respect to the filter parameters. This results in a set of M linear equations of the form

$$\sum_{k=1}^{M} \alpha(k) r_{uu}(k-1) = r_{pu}(l) - r_{uu}(l); \qquad l = 1, 2, \ldots, M \tag{33}$$

where the r_{uu} is the autocorrelation of $u(t)$ given by

$$r_{uu}(m) = \sum_{t=0}^{n} u(t) u(t-m) \tag{34}$$

and $r_{pu}(m)$ is the cross correlation of $p(t)$ and $u(t)$ given by

$$r_{pu}(m) = \sum_{t=0}^{n} p(t) u(t-m) \tag{35}$$

Note that $u(t) = 0$ for $t < 0$. Also $r_{uu}(m) = r_{uu}(-m)$. As a result, (33) may be written as

$$\begin{bmatrix} r_{uu}(0) & r_{uu}(1) & r_{uu}(2) & \cdots & r_{uu}(M-1) \\ r_{uu}(1) & r_{uu}(0) & r_{uu}(1) & \cdots & r_{uu}(M-2) \\ \vdots & \vdots & \vdots & & \\ r_{uu}(M-1) & r_{uu}(M-2) & r_{uu}(M-3) & \cdots & r_{uu}(0) \end{bmatrix} \begin{bmatrix} \alpha(1) \\ \alpha(2) \\ \vdots \\ \alpha(M) \end{bmatrix} = \begin{bmatrix} r_{pu}(1) - r_{uu}(1) \\ r_{pu}(2) - r_{uu}(2) \\ \vdots \\ r_{pu}(M) - r_{uu}(M) \end{bmatrix} \tag{36}$$

Equation (36) can be rewritten as

$$R\bar{\alpha} = \bar{r} \tag{37}$$

where the definitions of the matrix R, and the vectors $\bar{\alpha}$ and $\bar{r}$ are obvious from equation (36). Note that R is in Toeplitz form. The equation of the form (37) can be solved in a variety of ways to obtain the α parameters of the inverse transfer function. The most straightforward way conceptually is to invert the R matrix to get

$$\bar{\alpha} = R^{-1} \bar{r} \tag{38}$$

Recall, that the lattice filter is described by the following set of well known order-recursive equations described earlier, but repeated here

$$f_0(n) = g_0(n) = u(n) \tag{39}$$

$$f_m(n) = f_{m-1}(n) + \mu_m g_{m-1}(n-1)\ m = 1,2,\ldots,M \tag{40}$$

$$g_m(n) = \mu_m f_{m-1}(n) + g_{m-1}(n-1)\ m = 1,2,\ldots M \tag{41}$$

$$p(n) = f_M(n) \tag{42}$$

The lattice filter is equivalent to the FIR filter. As a result,

$$p(n) = f_M(n) = \sum_{k=0}^{M} \alpha(k)u(n-k)\ \alpha(0) = 1 \tag{43}$$

Indeed after any stage m of the. lattice, the $f_m(n)$ may be represented as

$$f_m(n) = \sum_{k=0}^{m} \alpha_m(k)u(n-k) \qquad \alpha(0) = 1 \tag{44}$$

where $\alpha_m(k)$'s are unique for each $0 < m \leq M$. Define

$$A_m(z) = 1 + \sum_{k=1}^{m} \alpha_m(k)z^{-k} \geq 1 \tag{45}$$

Then the z transform of (44) is

$$F_m(z) = A_m(z)U(z) \tag{46}$$

or

$$A_m(z) = \frac{F_m(z)}{U(z)} \tag{47}$$

Note $A_m(z)$ represents the transfer function from the input to the output, $f_m(n)$,after stage m. The other output g(n) may also be expressed as a sum. By working through equations (39) - (42), it seen that

$$g_m(n) = \sum_{k=0}^{m} \alpha_m(m-k)u(n-k) \tag{48}$$

where it is noted that the α 's needed for g(n) in (48) are the same as those needed for $f(n)$ in (44), but in reverse order. Define

$$B_m(z) = \sum_{k=0}^{m} \alpha_m(m-k)z^{-k} \tag{49}$$

Note

$$\text{Bin,(z)} = z^{-m}A_m(z^{-1}) \tag{50}$$

Then the z transform of (48) is

$$\text{G“,(z)} = B_m(z)U(z) \tag{51}$$

and

$$B_m(z) = \frac{G_m(z)}{U(z)} \tag{52}$$

Now take the z transform of equations (39)- (42)

$$\mathbf{Fe(z)} = G_0(z) = U(z) \tag{53}$$

$$F_m(z) = F_{m-1}(z) + \mu_m z^{-1}G_{m-1}(z)\ m = 1,2,\ldots,M \tag{54}$$

$$G_m(z) = \mu_m F_{m-1}(z)\ 4\ z^{-1}G_{m-1}(z)\ m = 1,2,\ldots,M \tag{55}$$

$$P(z) = F_M(z) \tag{56}$$

By dividing each equation by $U(z)$,

$$A_0(z) = B_0(z) = 1 \tag{57}$$

$$A_m(z) = A_{m-1}(z) + \mu_m z^{-1} B_{m-1}(z) \quad m = 1, 2, \ldots, M \tag{58}$$

$$B_m(z) = \mu_m A_{m-1}(z) + z^{-1} B_{m-1}(z) \quad m = 1, 2, \ldots, M \tag{59}$$

where $A_M(z)$ becomes the FIR transfer function. These equations an now be put into order recursive matrix form as

$$\begin{bmatrix} A_m(z) \\ B_m(z) \end{bmatrix} = \begin{bmatrix} 1 & \mu_m \\ \mu_m & 1 \end{bmatrix} \begin{bmatrix} A_{m-1}(z) \\ z^{-1} B_{m-1}(z) \end{bmatrix} \tag{60}$$

in order 1,0 directly compare the recursive matrix equation (60) tc the bar equations, (60) is now put into a slightly different form. Define

$$Q_m^-(z) = z^{-(m+1)} A_m(z^{-1}) \tag{61}$$

and

$$Q_m^+(z) = A_m(z) \tag{62}$$

By using these definitions in (58) and (59) and writing the new equations in matrix form,

$$\begin{bmatrix} Q_m^+(z) \\ Q_m^-(z) \end{bmatrix} = \begin{bmatrix} 1 & -\mu_m \\ -z^{-1}\mu_m & z^{-1} \end{bmatrix} \begin{bmatrix} Q_{m-1}^+(z) \\ Q_{m-1}^-(z) \end{bmatrix} \tag{63}$$

where from (57)

$$Q_0^+(z) = 1 \qquad Q_0^-(z) = -z^{-1}$$

A very elegant and efficient way of obtaining the reflection coefficients, μ_m, directly from (37) is to solve the Levinson-Durbin algorithm. In this algorithm, the α's are calculated recursively and the reflection coefficients are calculated as an intermediate step in the recursion. This method may be very useful in adaptively updating the reflection coefficients on-line.

APPENDIX B

Boundary Conditions and the Bar Equation

Let $u(x,t)$ be the axial displacement of a. bar element, where x is the distance variable in the axial direction and t is the time variable. For an axial bar element in which plane waves before deformation remain plane, $u(x,t)$ satisfies the wave equation given by

$$EA\frac{\partial^2 u(x,t)}{\partial x^2} = \rho A\frac{\partial^2 u(x,t)}{\partial t^2} \tag{64}$$

In this equation, E is the elastic. modulus, A *is* the cross sectional area, and ρ is the mass density. In more familiar wave equation form, (64) can be rewritten as

$$\frac{\partial^2 u(x,t)}{\partial x^2} = \frac{1}{c^2}\frac{\partial^2 u(x,t)}{\partial t^2} \tag{65}$$

where c is the wave speed, given by $c = \sqrt{\frac{E}{\rho}}$. This equation has the solution given earlier

$$u(x,t) = u^{+}(t - \frac{x}{c}) - u^{-}(t + \frac{x}{c}) \tag{66}$$

The axial force in the bar is related to the axial displacement by

$$p(x,t) = EA\frac{\partial u(x,t)}{\partial x} \tag{67}$$

Given the solution for the axial displacement, the axial force may be written as

$$p(x,t) = -j\omega\frac{EA}{c}u^{+}(t - \frac{x}{c}) - j\omega\frac{EA}{c}u^{-}(t + \frac{x}{c}) \tag{68}$$

From structural theory, both the displacement and the axial force must be continuous at each boundary. Consider the boundary at x_m between sections m and $m+1$, The continuous displacement condition is written as

$$u_{m+1}(x_m,t) = u_m(x_m,t) \tag{69}$$

or

$$u_m^{+}(t - \frac{x_m}{c}) - u_m^{-}(t + \frac{x_m}{c}) = u_{m+1}^{+}(t - \frac{x_m}{c}) - u_{m+1}^{-}(t + \frac{x_m}{c}) \tag{70}$$

Since the bar is assumed lossless, it is noted that the left traveling wave has the same amplitude at junction x_m and time t as the same left traveling wave at junction x_{m+1} at a time δt later. The same is true for the right traveling wave at a time δt earlier. Since each bar section is of equal length, $\delta t = \frac{\delta l}{\sqrt{\frac{E}{\rho}}}$. Therefore,

$$u_{m+1}^{-}(t + \frac{x_m}{c}) = u_{m+1}^{-}((t + \delta t) + \frac{x_{m+1}}{c}) = u_{m+1}^{-}(x_{m+1}, t + \delta t)$$

$$u_{m+1}^{+}(t - \frac{x_m}{c}) = u_{m+1}^{+}((t - \delta t) - \frac{x_{m+1}}{c}) = u_{m+1}^{+}(x_{m+1}, t - \delta t)$$

From these equations, it is seen that as long as the proper time is observed, u_{m+1} can always be measured at boundary x_{m+1}. Therefore, the distance subscript x can be dropped and the displacement continuity condition can be written in short form as

$$u_m^{+}(t) - u_m^{-}(t) = u_{m+1}^{+}(t - \delta t) - u_{m+1}^{-}(t + \delta t) \tag{71}$$

Similar to the continuous displacement condition, the continuous axial force condition is written as

$$p_{m+1}(x_m, t) = p_m(x_m, t) \tag{72}$$

This condition can be rewritten using (68) as

$$\frac{E_{m+1}A_{m+1}}{c}u^-_{m+1}(t+\frac{x_m}{c})+\frac{E_{m+1}A_{m+1}}{c}u^+_{m+1}(t-\frac{x_m}{c})=\frac{E_mA_m}{c}u^-_m(t+\frac{x_m}{c})+\frac{E_mA_m}{c}u^+_m(t-\frac{x_m}{c}) \tag{73}$$

By again using the lossless property of the bar,

$$E_{m+1}A_{m+1}u^-_{m+1}(t+\delta t)+E_{m+1}A_{m+1}u^+_{m+1}(t-\delta t)=E_mA_mu^-_m(t)+E_mA_mu^+_m(t) \tag{74}$$

In order to simplify the notation, let

$$S_m = E_mA_m$$

then (74) may be written as

$$S_{m+1}u^-_{m+1}(t+\delta t)+S_{m+1}u^+_{m+1}(t-\delta t)=S_mu^-_m(t)+S_mu^+_m(t) \tag{75}$$

With the use of (75) and (71)

$$u^-_{m+1}(t+\delta t)=\frac{1}{2}u^+_m(t)(1-\frac{S_m}{S_{m+1}})+\frac{1}{2}u^-_m(t)(1+\frac{S_m}{S_{m+1}}) \tag{76}$$

is obtained. Similarly, with the use of (75) and (71)

$$u^+_{m+1}(t-\delta t)=\frac{1}{2}u^+_m(t)(1+\frac{S_m}{S_{m+1}})-\frac{1}{2}u^-_m(t)(1-\frac{S_m}{S_{m+1}}) \tag{77}$$

Now define

$$\eta_m=\frac{E_{m+1}A_{m+1}-E_mA_m}{E_{m+1}A_{m+1}+E_mA_m}=\frac{S_{m+1}-S_m}{S_{m+1}+S_m} \tag{78}$$

Then (76) may be written as

$$u^-_{m+1}(t+\delta t)=\frac{1}{1+\eta_m}[u^-_m(t)-\eta_mu^+_m(t)] \tag{79}$$

and (77) may be written as

$$u^+_{m+1}(t-\delta t)=\frac{1}{1+\eta_m}[u^+_m(t)-\eta_mu^-_m(t)] \tag{80}$$